A Hybrid White Balance Method Integrating Pyramid-Based Multi-Scale and Sclera-Based Approaches

Yi-Ning Tu[*], Cheng-Xin Lin
Department of Statistics and Information Science, Fu Jen Catholic University, Taiwan (R.O.C.)

Keywords	Abstract
White Balance; Color Constancy; Pyramid-Based Multi-Scale Method; Block-Based Division; Sclera-Based Method	White balance is a key technique in image processing for restoring true object colors by correcting color casts caused by illumination. Traditional methods often fail under practical conditions, while sclera-based approaches are affected by complex lighting, and pyramid-based multi-scale block methods lack stable brightness references. To address these issues, this study proposes a Hybrid White Balance Method combining multi-scale color correction with sclera-based brightness compensation. Experiments were conducted using 288 filtered images generated from 72 original face images under four lighting conditions (cool/warm tone, bright/dim). Performance was evaluated with CIEDE2000 (ΔE_{00}), comparing six white balance methods. Results show that the Hybrid Method achieved the lowest average ΔE_{00} (5.25) across the dataset, significantly outperforming other methods. Moreover, it consistently reduced outliers, demonstrating superior accuracy and stability under diverse lighting conditions.

1. Introduction

With the rapid advancement of computer vision and its growing applications in fields such as medical imaging, surveillance, augmented reality (AR), and virtual reality (VR), the need for accurate image color representation has become increasingly critical. However, inconsistent lighting conditions frequently introduce color casts that compromise image quality. To address this, white balance techniques are employed in image processing to correct color distortions and restore the true colors of objects.

Traditional white balance methods based on global assumptions—such as the Gray-World and White-Patch methods—often fail in complex environments. More advanced techniques, like the Pyramid-Based Method and Sclera-Based Method, offer improvements by addressing tone and brightness, respectively. Yet, each has limitations when used alone. This study proposes a

---

*corresponding author. Email: eniddu@gmail.com

hybrid white balance method that integrates both approaches to enhance correction accuracy and adaptability under diverse lighting conditions. The aim is to develop, implement, and evaluate this method against traditional techniques to verify its effectiveness in improving image color consistency.

2. Literature Review

Color balance aims to restore natural image colors by estimating and correcting the influence of light sources (Chen & Zhang, 2015). However, variations in lighting, such as low-temperature incandescent or high-temperature daylight, often cause color casts that degrade image quality (Dhara et al., 2021). Traditional methods like the Gray-World Assumption (Buchsbaum, 1980), White-Patch Method (Land & McCann, 1971), and Max-RGB (Barnard et al., 2002) are based on global assumptions but fail under uneven or multi-light scenarios (Provenzi et al., 2008; Cheng et al., 2014).

To improve robustness, region-based techniques were introduced. Face-based approaches estimate illumination using skin tone (Bianco & Schettini, 2012, 2014), while sclera-based methods utilize the stable reflectance of sclera (Males et al., 2017; Choi et al., 2017), offering greater consistency. As a biologically grounded and reliable reference point, the sclera serves as a more advanced alternative to earlier reference-based methods such as the White-Patch and Max-RGB methods, which rely on the brightest region or channel maximum. However, it is still vulnerable to detection errors or individual variability.

Multi-scale techniques like the Multi-Scale Retinex (Jobson, Rahman, & Woodell, 1995; Jobson et al., 1997) enhance both detail and balance, and the Pyramid-Based Multi-Scale Block Method (Ulucan et al., 2023, 2024) further improves adaptability by estimating lighting using the top 3.8% brightest pixels, Gaussian weighting, and block division, making it effective in uneven lighting conditions. It builds on the Gray-World assumption of globally balancing RGB and incorporates reference concepts from the White-Patch and Max-RGB methods, making it a refined extension of all three. However, it still lacks a biologically consistent reference like the sclera, which limits its stability in complex scenes.

Through practical implementation in this study, it was observed that the sclera-based method offers stable brightness correction by leveraging the consistent reflectance of the sclera, though it is less effective in tone adjustment. In contrast, the pyramid-based method performs well in correcting color tone but lacks a reliable standard for brightness adjustment. Therefore, this study proposes a hybrid white balance method that integrates the pyramid-based method for tone correction and the sclera-based method for brightness adjustment, offering a more comprehensive and robust solution in complex lighting environments.

3. Methodology

This study aims to enhance image white balance by integrating the Pyramid-Based Multi-Scale Block Method with the Sclera-Based Method into a novel "Hybrid Method." As shown in Fig. 1, the overall research framework consists of the following main steps:

Step 1. Data preprocessing: Collect N original images as the sample dataset. Each original image is augmented with four different filters to simulate varying lighting conditions, producing 4N filtered images. The filters include "cool-bright," "cool-dim," "warm-bright," and "warm-dim." Subsequently, the eye regions of these 4N filtered images (N for each filter) are extracted using YOLO.

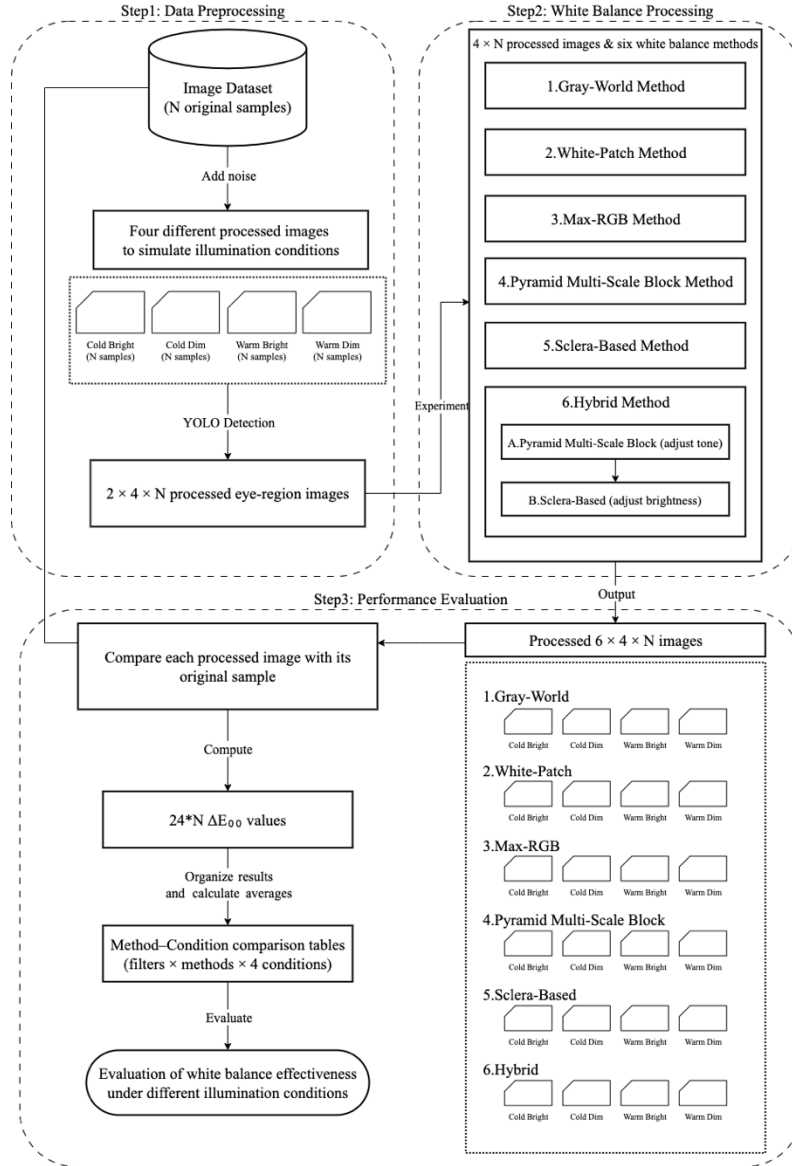**Fig. 1** *Research Framework*

Step 2. White balance processing: Apply six white balance methods to the 4N filtered images: the Gray-World method, White-Patch method, Max-RGB method, Pyramid-Based Multi-Scale Block method, Sclera-Based method, and the proposed Hybrid Method. In the

Hybrid Method, the Pyramid-Based approach is first used for color tone adjustment, followed by the Sclera-Based approach for brightness correction, resulting in white-balanced images refined in two stages. In total, applying six methods to 4N filtered images produces 24N processed images.

Step 3. Performance evaluation: Each of the 24N processed images is compared pixel-wise with its corresponding original image, producing 24N ΔE_{00} values. These values are categorized into 24 filter–method combinations, with each combination containing N ΔE_{00} values from different original samples. The average ΔE_{00} is then calculated for each combination, resulting in 24 average values. By comparing the average ΔE_{00} across six methods under four filter conditions, the effectiveness of each method in different lighting scenarios is evaluated.

3.1 Data Preprocessing

The images used in this study were required to contain a complete human face with clear facial features and unobstructed scleral regions, ensuring reliable analysis of illumination effects on scleral color characteristics. To qualify, images had to meet two criteria: (1) facial features must be sharp and discernible, and (2) scleral regions must be free from overexposure and shadow occlusion.

Each image was further processed with four filters representing different lighting conditions—cool-bright, cool-dim, warm-bright, and warm-dim, as illustrated in Fig. 2(A)—constructed through a two-dimensional design varying in brightness and color temperature. The warm-dim condition is used as an illustrative example in subsequent sections. Eye regions were extracted using the YOLOv7 detection model, as shown in Fig. 2(B), which provided bounding boxes for the eyes. A sample cropped eye under the warm-dim filter is presented in Fig. 2(C). All images were organized by filter type to prepare reliable input for the sclera-based white balance method.
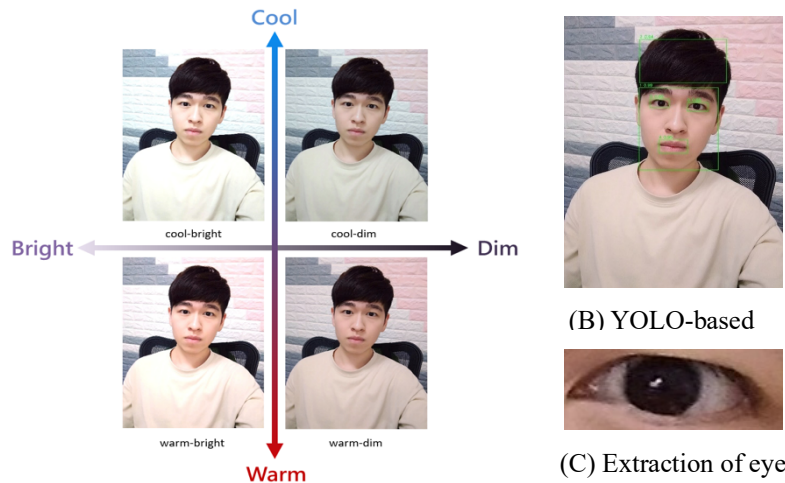

Fig. 2 *Data Preprocessing Pipeline. (A) Four types of lighting filters applied to each facial image, varying across brightness and color temperature (cool-bright, cool-dim, warm-bright, warm-dim). (B) Facial and eye detection performed using a YOLO-based model. (C) Extracted eye region used for sclera-based brightness correction.*

3.2 Pyramid-Based Method

The Pyramid-Based Multi-Scale Block Method serves as the tone correction module of the proposed Hybrid White Balance framework. It is designed to improve illumination color estimation, particularly under non-uniform or multi-source lighting conditions. By integrating multi-scale pyramid analysis with block-based partitioning, the method captures both global and local image features, thereby achieving more accurate illumination estimation and correction.

At the theoretical level, the pyramid representation enables progressive downsampling of the image, preserving fine details at higher resolutions while summarizing global illumination trends at lower resolutions. In parallel, block partitioning divides each pyramid level into uniform regions, within which illumination is estimated independently. This dual design enhances the adaptability of the method to spatially varying illumination.

Following Ulucan et al. (2024), the workflow of the method comprises the extraction of bright regions, Gaussian-based weighting to suppress noise, block-wise illumination estimation, and the integration of estimates across multiple pyramid layers. Within each block, the illumination estimate is computed as a weighted average of pixel values, as shown in Equation (3.1).

$$C_{\text{block}} = \frac{\sum_{(x,y) \in \text{Bright part}} I(x,y) \cdot W_s(x,y) \cdot W_l(x,y)}{\sum_{(x,y) \in \text{Bright part}} W_s(x,y) \cdot W_l(x,y)} \tag{3.1}$$

where $I(x,y)$ represents the RGB values of a pixel, $W_s(x,y)$ denotes the spatial weighting factor, and W_l denotes the luminance-based weighting factor. The illumination estimates of all valid blocks in a given layer are then averaged as shown in Equation (3.2):

$$C_{\text{layer}} = \frac{1}{n} \sum_{i=1}^{n} C_{block,i} \tag{3.2}$$

In this formulation, C_{layer} denotes the illumination color estimate of the given pyramid layer, while C_{block} represents the illumination color estimate obtained from each valid block. The variable n refers to the total number of blocks containing bright pixels, which are included in the averaging process.

After the illumination color estimation of the original image is completed, a pyramid structure is constructed using the *pyrDown* function in OpenCV, which reduces the resolution by half at each level. The process continues until the image becomes too small to be partitioned into the predefined set of 120 blocks. In the sample case, this limitation occurred at the ninth level, resulting in a final effective depth of eight layers (Fig. 3).

Each pyramid layer undergoes the aforementioned steps, including bright region extraction, Gaussian smoothing based on luminance, block partitioning, spatial Gaussian weighting within each block, and illumination color estimation for that layer. This process enables multi-scale analysis of image features at different resolutions, as illustrated in Fig. 4(A). The illumination color estimates from all layers are then averaged to obtain the final illuminant estimate C_{final} as defined in Equation (3.3). In this context, C_{final} denotes the final estimated illuminant, while C_{layer} represents the illumination estimate of a single pyramid layer. The variable n refers to the total number of pyramid layers used in the computation.
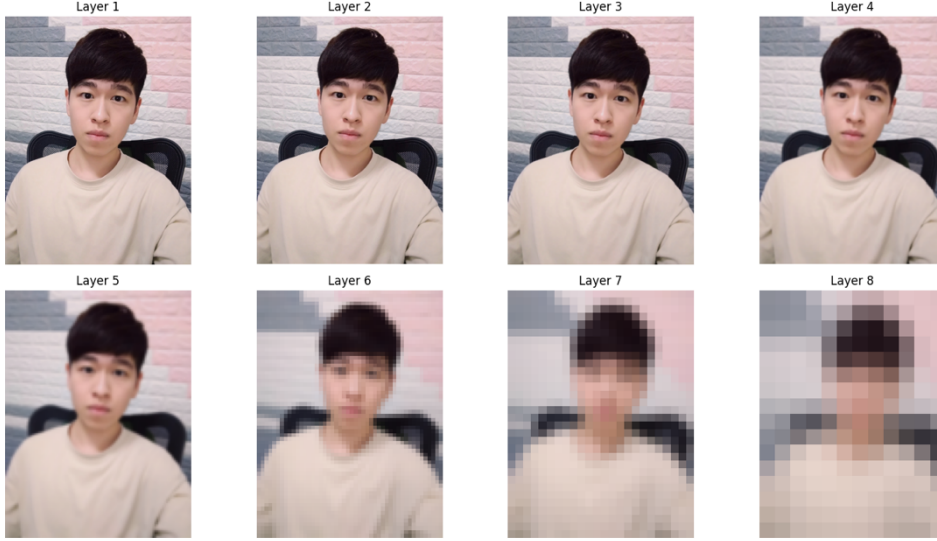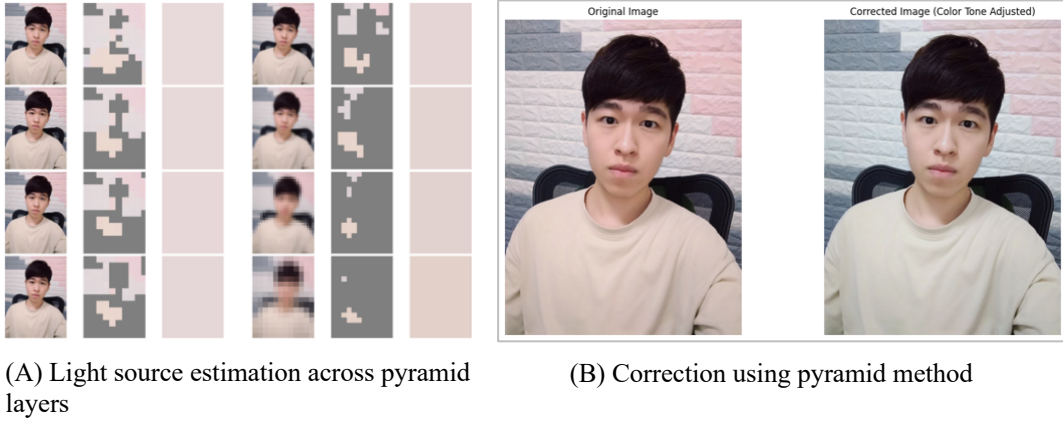
Fig. 3 *Illustration of Pyramid-Based Images Across Multiple Levels*

(A) Light source estimation across pyramid layers

(B) Correction using pyramid method

Fig. 4 *Tone Correction Using the Pyramid-Based Method. (A) Multi-scale light source estimation across pyramid layers, with the final global illuminant (corresponding to Equation (3.3)) shown on the right. (B) Before-and-after comparison of tone correction, where the original warm-dim image shows a reddish cast and the corrected version appears more natural and closer to neutral white.*

$$C_{final} = \frac{1}{n}\sum_{i=1}^{n} C_{\text{layer}} \tag{3.3}$$

The final illuminant estimate C_{final} is applied to global tone correction of the image. To align the image tone with the predefined target illuminant T, the RGB channel values of each pixel are adjusted according to their proportional relationship with C_{final}. The adjustment is defined as shown in Equation (3.4):

$$I_{\text{corrected}}(x,y) = I(x,y) \times \frac{T/C_{final}}{\text{mean}(T/C_{final})} \tag{3.4}$$

Where $I(x, y)$denotes the original RGB pixel value at position (x,y); T: represents the target illuminant, typically set to neutral white; and C_{final} is the illuminant estimated by the pyramid-based method. The term T / C_{final} indicates the channel-wise ratio between the target and estimated illuminants, while mean(T / C_{final}) corresponds to the average of the three channel ratios, which serves as a normalization factor to preserve overall brightness.

All images were preprocessed by normalizing the original sRGB values to the [0,1] range and converting them into a linear color space via gamma correction. The number of blocks per layer was set to approximately 120, and the pyramid was constructed until further partitioning became unstable. An illustrative example using a warm-dim filtered image is shown in Fig. 4(B). the original image exhibits a reddish cast, whereas the corrected version appears more natural and closer to neutral white, demonstrating the effectiveness of the Pyramid-Based Multi-Scale Block Method in reducing color bias while preserving brightness.

3.3 Sclera-Based Method

Following tone correction by the pyramid-based method, the sclera-based method adjusts brightness by leveraging the sclera's high reflectance and low saturation. As illustrated in Fig. 5, the extraction process involves filtering out high-saturation areas in HSL space, applying thresholding to generate a low-saturation mask, and finally selecting the brightest pixels as the sclera-based bright region.

To perform brightness correction, the average brightness of the extracted regions was first computed for each image, as shown in Fig. 6(A). These values were then averaged to derive a global target brightness (Fig. 6(B)), which serves as the normalization reference. The brightness of the selected region in the current image (Fig. 6(C)) is then compared with the target, and the image is rescaled accordingly, as expressed in Equation (3.5):

$$I_i'(x,y) = I_i(x,y) \times \frac{\text{Target}_{\text{Brightness}}}{\text{Brightness}_i} \tag{3.5}$$

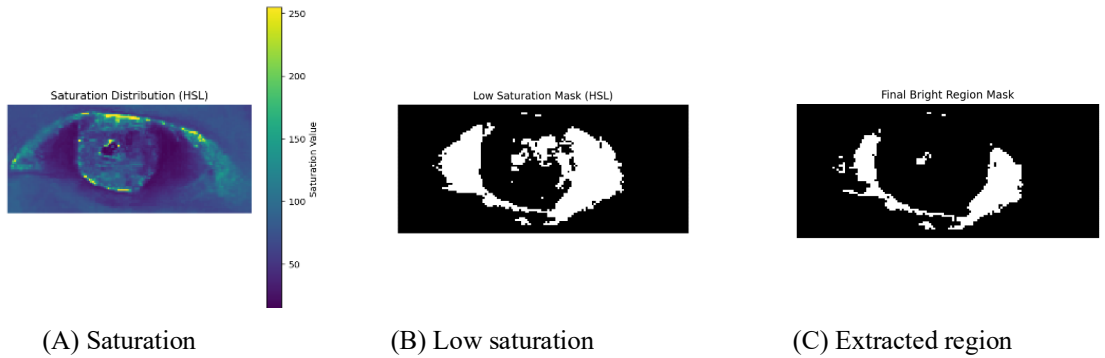|		
(A) Saturation	(B) Low saturation	(C) Extracted region

Fig. 5 *Extraction Process of the Sclera-Based Bright Region. (A) Saturation distribution in HSL color space. (B) Low-saturation binary mask after thresholding. (C) Final extracted bright region mask used for brightness correction.*
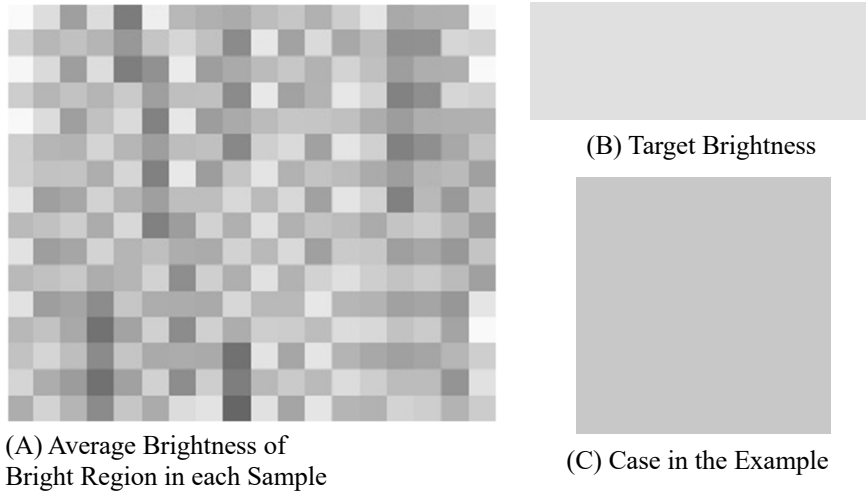
(A) Average Brightness of
Bright Region in each Sample

(B) Target Brightness

(C) Case in the Example

Fig. 6 *Brightness Reference Calculation for Sclera-Based Correction. (A) Average brightness values of the bright regions extracted from each sample. (B) Computed target brightness, obtained as the overall average across all samples. (C) Bright region brightness of the current example image before correction.*

3.4 Evaluation of the Hybrid White Balance Method

This section evaluates the proposed Hybrid Method, which combines tone correction (Pyramid-Based Method) and brightness adjustment (Sclera-Based Method) for improved color restoration under various lighting conditions. The overall workflow of the evaluation process is illustrated in Fig. 7.
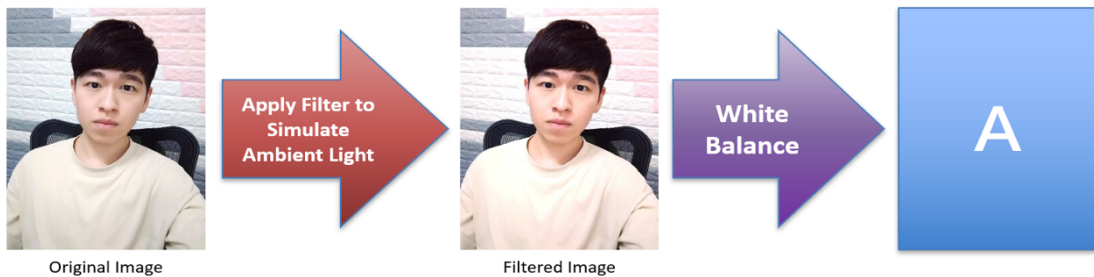

Original Image — Apply Filter to Simulate Ambient Light — Filtered Image — White Balance — A

Fig. 7 *Overall Workflow of White Balance Correction. The original image is first processed with a simulated lighting filter to generate a filtered image. A white balance algorithm is then applied to correct the color cast and restore natural appearance. Block A represents the output of any white balance method under evaluation.*

Table 1 presents a visual comparison of three key stages under the warm-dim filter condition: the original image after filtering (Pre-adjusting), the intermediate result after tone correction (Pyramid-Only), and the final output after both tone and brightness correction (Full Hybrid). The fully corrected image appears the most natural, indicating that the two-stage correction strategy effectively removes color cast and restores visual realism. To quantitatively assess performance, the Mean Absolute Percentage Error (MAPE) is used, as defined in Equation (3.6):

$$MAPE = \frac{1}{n}\sum_{i=1}^{n}\left|\frac{O_i - A_i}{O_i}\right| \times 100 \tag{3.6}$$

Table 1 *Visual Comparison of Hybrid White Balance Results under Warm-Dim Filter*

Filter Type	Pre-adjusting	Pyramid-Only	Full Hybrid
Warm-Dim			

Under the warm-dim condition, the Hybrid Method achieved a MAPE of 2.70, reflecting high accuracy even in low-light, warm-toned scenarios. To validate its robustness, the Hybrid Method is compared against five classical methods. If the Hybrid Method consistently shows the lowest MAPE values, it will confirm its effectiveness in tone and brightness correction.

In addition to using MAPE, this study assumes that the original image represents the ground truth, while the filtered images simulate the appearance of the original under various lighting conditions. The objective of white balance is to restore the filtered image to its original form. Let A denote the result obtained after applying a white balance method; the similarity between A and the original image serves as a measure of the white balance performance, with higher similarity indicating better performance. Furthermore, this study employs the widely used CIEDE2000 (ΔE_{00}) color-difference metric, originally proposed by Luo, Cui, and Rigg (2001), as an additional indicator, with its calculation formula shown in Equation (3.7).

$$\Delta E_{00} = \sqrt{\left(\frac{\Delta L'}{k_L S_L}\right)^2 + \left(\frac{\Delta C'}{k_C S_C}\right)^2 + \left(\frac{\Delta H'}{k_H S_H}\right)^2 + R_T \frac{\Delta C'}{k_C S_C}\frac{\Delta H'}{k_H S_H}} \tag{3.7}$$

where $\Delta L'$, $\Delta C'$, and $\Delta H'$ denote the differences in lightness, chroma, and hue, respectively, before and after correction; S_L, S_C, and S_H are the weighting functions for lightness, chroma, and hue; k_L, k_C, and k_H are the parametric factors, typically set to 1 under standard experimental conditions; and R_T is the rotation term that accounts for the interaction between chroma and hue, which further improves accuracy in the critical regions of hue. A lower ΔE_{00} value indicates

a smaller difference between the white-balanced result and the original image, thereby reflecting better white balance performance. ΔE_{00} captures both lightness and chromatic differences, and it has been calibrated through human visual perception experiments, making it a more faithful representation of visual experience.

4. Experimental Results

A total of 72 color face images with clearly visible scleral regions were collected to support illumination estimation and brightness compensation. The dataset was balanced by gender (36 male, 36 female), and all images were obtained from publicly available sources (Google Images) for academic use. Basic characteristics, including resolution, grayscale intensity, HSL saturation, and RGB channels, were quantified and visualized. Preprocessing involved automated filter simulation, standardized naming, and YOLO-based eye cropping, producing 288 high-resolution eye images. Representative scleral pixels were then extracted using a low-saturation, high-brightness strategy to establish a consistent brightness reference.

To ensure consistent evaluation, each of the 72 original images was processed with four filters (cool/warm × bright/dim), yielding 288 filtered samples. A standardized naming scheme facilitated automated batch processing and file management. Eye regions were localized and cropped using the YOLOv7 detection model, with the higher-resolution crop retained, resulting in 288 high-quality eye images for analysis.

In the brightness compensation stage of the Hybrid Method, scleral bright pixels were extracted based on a low-saturation and high-brightness strategy, reflecting the stability and neutrality of the sclera. For each image, the mean RGB value of the scleral region was calculated, and the overall averages across all 288 samples defined the target scleral color, TargetRGB = (188.03, 163.21, 155.12). Since only brightness adjustment was required, the average of these three channels (TargetBrightness $\approx$ 168.79) was used as the global reference. Images were then linearly adjusted according to the deviation between their actual scleral brightness and this target, providing a consistent and reliable baseline for correction.

Table 2 compares the average MAPE values of six white balance methods across the four filter conditions. The proposed Hybrid Method achieved the lowest overall average MAPE (9.69), outperforming both traditional approaches (Gray-World, White-Patch, Max-RGB) and advanced methods (Pyramid-Based, Sclera-Based). Table 3 presents paired t-tests between the Hybrid Method and each of the other five methods. The improvements achieved by the Hybrid Method were statistically significant ($p < 0.05$), confirming its effectiveness. Table 4 reports MAPE distribution statistics for each method. The Hybrid Method yielded the lowest median value (9.24) and the fewest outliers (2; 0.69%), demonstrating not only high accuracy but also strong consistency across different lighting conditions.

In addition to MAPE, this study further employed the perceptually calibrated CIEDE2000 (ΔE_{00}) color-difference metric to evaluate visual similarity between corrected and original images. Table 5 summarizes the average ΔE_{00} values of six methods across the four filter conditions. Among these, the Hybrid Method consistently achieved the lowest ΔE_{00} values, with the warm-bright condition showing the best performance. These results further confirm the Hybrid Method's superiority in restoring natural colors under diverse and complex lighting environments.

Table 2 *MAPE Comparison of White Balance Methods by Filter Type*

Filter Type	Gray-World	White-Patch	Max-RGB	Pyramid-Based	Sclera-Based	Hybrid
Cool-Bright	10.98	12.72	13.72	11.52	10.25	9.55
Cool-Dim	11.63	9.65	7.68	10.11	10.34	9.71
Warm-Bright	10.3	12.43	13.43	10.63	10.5	9.82
Warm-Dim	12.18	9.67	7.81	10.8	10.28	9.69
Average	11.27	11.12	10.66	10.77	10.34	9.69

Values in red represent the results of the proposed Hybrid method. Bold values indicate the average MAPE across all lighting types.

Table 3 *Paired t-Test Results Between the Hybrid Method and Other White Balance Methods*

Comparison Pair	t-value	p-value	Significance
Hybrid vs. Gray-World	-5.18	4.11E-07	Significant difference
Hybrid vs. White-Patch	-3.24	0.0013	Significant difference
Hybrid vs. Max-RGB	-2.26	0.0243	Significant difference
Hybrid vs. Pyramid-Based	-3.4	0.0008	Significant difference
Hybrid vs. Sclera-Based	-4.68	4.34E-06	Significant difference

Table 4 *MAPE Distribution Statistics for Each White Balance Method*

White Balance Method	Q1	Median	Q3	IQR	Std. Dev.	Outlier Count	Outlier Rate
Gray-World	9.50	11.07	12.14	2.64	2.60	18	6.25%
White-Patch	7.60	9.82	13.13	5.53	6.24	22	7.64%
Max-RGB	6.50	10.18	12.54	6.04	5.79	18	6.25%
Pyramid-Based	8.89	10.12	11.57	2.68	3.20	19	6.60%
Sclera-Based	7.59	9.40	12.15	4.56	4.72	13	4.51%
Hybrid (Proposed)	6.42	9.24	12.33	5.91	4.67	2	0.69%

Table 5 *Average ΔE_{00} (%) of Six White Balance Methods under Four Filter Conditions*

Filter Type	Gray-World	White-Patch	Max-RGB	Pyramid-Based	Sclera-Based	Hybrid (Proposed)
Cool-Bright	7.38	7.20	7.20	5.92	5.67	5.16
Cool-Dim	7.95	6.46	5.61	6.07	5.61	5.25
Warm-Bright	7.20	7.27	7.27	5.58	5.83	5.33
Warm-Dim	8.13	6.48	5.66	6.32	5.58	5.24
Average	7.66	6.85	6.44	5.97	5.67	5.25

5.   Conclusions

This study proposed a Hybrid Method that integrates the Pyramid-Based Multi-Scale Block Method with the Sclera-Based Method to address white balance challenges under varying color temperature and brightness conditions. By combining tone correction with brightness compensation, the proposed approach enhances both accuracy and stability. Experiments conducted under four simulated lighting conditions (cool-bright, cool-dim, warm-bright, warm-dim) demonstrated that the Hybrid Method consistently outperformed its constituent methods as well as traditional baselines. It achieved the lowest average ΔE_{00} values across 288 samples, with paired t-tests confirming statistically significant improvements ($p < 0.05$). Error analysis further highlighted its robustness, revealing fewer outliers and reduced variability, even under dim or biased lighting. In summary, the Hybrid Method effectively integrates complementary techniques to provide accurate, stable, and reliable white balance correction, demonstrating strong adaptability and practical potential for real-world imaging applications.

References

Barnard, K., Cardei, V., & Funt, B. V. (2002). A comparison of computational color constancy algorithms—Part I: Methodology and experiments with synthesized data. *IEEE Transactions on Image Processing, 11*(9), 972–984. https://doi.org/10.1109/TIP.2002.802531

Bianco, S., & Schettini, R. (2012). Color Constancy Using Faces. *Proceedings of the IEEE Computer Society Conference on Computer Vision and Pattern Recognition (CVPR)*, 65–72. DOI: 10.1109/CVPR.2012.6247659

Bianco, S., & Schettini, R. (2014). Adaptive color constancy using faces. *IEEE Transactions on Pattern Analysis and Machine Intelligence, 36*(8), 1505–1519. https://doi.org/10.1109/TPAMI.2013.2297710

Buchsbaum, G. (1980). A spatial processor model for object color perception. *Journal of the Franklin Institute, 310*(1), 1–26. https://doi.org/10.1016/0016-0032(80)90058-7

Chen, G., & Zhang, X. (2015). A method to improve robustness of the gray world algorithm. In *4th International Conference on Computer, Mechatronics, Control and Electronic Engineering (ICCMCEE)* (pp. 250–255). Atlantis Press. https://doi.org/10.2991/iccmcee-15.2015.46

Cheng, D., Prasad, D. K., & Brown, M. S. (2014). Illuminant estimation for color constancy: Why spatial-domain methods work and the role of the color distribution. *Journal of the Optical Society of America A, 31*(5), 1049–1058. https://doi.org/10.1364/JOSAA.31.001049

Choi, H., Choi, K., & Suk, H. J. (2017). The human sclera and pupil as the calibration targets. *Electronic Imaging, 29*(17), 200–203. DOI: 10.2352/ISSN.2470-1173.2017.17.COIMG-448

Dhara, S. K., Roy, M., Sen, D., & Biswas, P. K. (2021). Color Cast Dependent Image Dehazing via Adaptive Airlight Refinement and Non-linear Color Balancing. *IEEE Transactions on Circuits and Systems for Video Technology, 31*(5), 2076–2081. https://doi.org/10.1109/TCSVT.2020.3007850

Jobson, D. J., Rahman, Z., & Woodell, G. A. (1995). Properties and performance of a center/surround retinex. *IEEE Transactions on Image Processing, 6*(3), 451–462. 10.1109/83.557356

Jobson, D. J., Rahman, Z., & Woodell, G. A. (1997). A multiscale retinex for bridging the gap between color images and the human observation of scenes. *IEEE Transactions on Image Processing, 6*(7), 965–976. https://doi.org/10.1109/83.597272

Land, E. H., & McCann, J. J. (1971). Lightness and Retinex Theory. *Journal of the Optical Society of America, 61*(1), 1–11. https://doi.org/10.1364/JOSA.61.000001

Luo, M. R., Cui, G., & Rigg, B. (2001). The development of the CIE 2000 colour-difference formula: CIEDE2000. *Color Research & Application, 26*(5), 340–350. https://doi.org/10.1002/col.1049

Males, M., Hedi, A., & Grgic, M. (2018). Colour balancing using sclera colour. *IET Image Processing, 12*(3), 416–421. https://doi.org/10.1049/iet-ipr.2017.0182

Provenzi, E., Gatta, C., Fierro, M., & Rizzi, A. (2008). A spatially variant white-patch and gray-world method for color image enhancement driven by local contrast. *IEEE Transactions on Pattern Analysis and Machine Intelligence, 30*(10), 1757–1770. https://doi.org/10.1109/TPAMI.2007.70827

Ulucan, O., Ulucan, D., & Ebner, M. (2023). Multi-Scale Block-Based Color Constancy. *Proceedings of the 31st European Signal Processing Conference (EUSIPCO),* 536–540. https://doi.org/10.23919/EUSIPCO58844.2023.10290103

Ulucan, O., Ulucan, D., & Ebner, M. (2024). Multi-scale color constancy based on salient varying local spatial statistics. *The Visual Computer, 40*(7), 5979–5995. https://doi.org/10.1007/s00371-023-03148-7

Yi-Ning Tu
Department of Statistics and Information Science, Fu Jen Catholic University, Taiwan(R.O.C.)
E-mail address: eniddu@gmail.com
Major area(s): Data Mining, Text Mining, Artificial Intelligence, Machine Learning, Information Retrieval

Cheng-Xin Lin
Department of Statistics and Information Science, Fu Jen Catholic University, Taiwan(R.O.C.)
E-mail address: x56572000@gmail.com
Major area(s): Data Mining, Machine Learning